Acta Crystallographica Section D
Biological Crystallography
ISSN 0907-4449

Leishmania mexicana mexicana glucose-6-phosphate isomerase: crystallization, molecular-replacement solution and inhibition

Artur T. Cordeiro,[a] Renaud Hardré,[b] Paul A. M. Michels,[c] Laurent Salmon,[b] Luis F. Delboni[d] and Otavio H. Thiemann[a]*

[a]Laboratory of Protein Crystallography and Structural Biology, Physics Institute of São Carlos, University of São Paulo, USP, Av. Trabalhador Sãocarlense 400, PO Box 369, 13566-590 São Carlos-SP, Brazil, [b]Laboratoire de Chimie Bioorganique et Bioinorganique, CNRS–UMR 8124, Institut de Chimie Moléculaire et des Matériaux d'Orsay, Université Paris-Sud XI, 91405 Orsay CEDEX, France, [c]Research Unit for Tropical Diseases and Laboratory of Biochemistry, Christian de Duve Institute of Cellular Pathology, Avenue Hippocrate 74, 1200 Brussels, Belgium, and [d]Pontificia Universidade Católica de Minas Gerais, Campus de Poços de Caldas, Av. Padre Francis Cletus Cox 1661, 37701-355 Poços de Caldas-MG, Brazil

Correspondence e-mail: thiemann@if.sc.usp.br

Received 13 August 2003
Accepted 17 February 2004

Glucose-6-phosphate isomerase (PGI; EC 5.3.1.9; also often called by its old nomenclature phosphoglucose isomerase) is an intracellular enzyme that catalyses the reversible conversion of D-glucose 6-phosphate (G6P) to D-fructose 6-phosphate (F6P). The native *Leishmania* PGI is a homodimeric molecule of 60 kDa per monomer with 47% sequence identity to human PGI. It has been shown to be present in both the cytosol and the glycosome of *Leishmania* promastigotes and represents a potential target for rational drug design. The present work describes the crystallization of two bacterially expressed *Leishmania* PGI constructs, one corresponding to the natural protein and the other to an N-terminally deleted form. Crystals of both forms are identical and present a large *c* unit-cell parameter. A complete data set was collected from the N-terminally deleted PGI to a resolution of 3.3 Å in space group $P6_1$, with unit-cell parameters $a = b = 87.0$, $c = 354.7$ Å, $\alpha = \beta = 90$, $\gamma = 120^\circ$. A preliminary study of the first inhibitors to be evaluated on the *Leishmania* enzyme is also reported.

1. Introduction

Glucose-6-phosphate isomerase (PGI; EC 5.3.1.9) is an intracellular enzyme that catalyzes the reversible conversion of D-glucose 6-phosphate (G6P) to D-fructose 6-phosphate (F6P). This isomerization reaction is a common step in the glycolytic, gluconeogenesis and pentose-phosphate pathways.

PGI has been studied in the Kinetoplastida as a potential target for the design of novel inhibitors because of the differences between the host (human) and parasitic glycolytic pathways and the dependence of the parasite on glycolysis. Recently, RNA-interference (RNAi) studies have revealed that decreasing the level of PGI in bloodstream-form *Trypanosoma brucei* PGI results in a 50% growth inhibition (Readmond *et al.*, 2003). This result is indicative of the central role that PGI plays in the parasite metabolism.

In *Leishmania mexicana mexicana* promastigotes, PGI activity is mainly (90%) detected in the cytosol and the remainder is localized to peroxisome-like organelles called glycosomes. The PGI activity in the two compartments could not be attributed to different isoenzymes owing to protein similarity and a single PGI gene is present in the haploid genome (Nyame *et al.*, 1994). Glycosomes are present in all Kinetoplastida and are known to compartmentalize the first seven enzymes of the glycolytic pathway with important consequences for the regulation of the glycolytic flux (Michels *et al.*, 2000).

PGI catalytic residues are well conserved in *L. mexicana*, *T. cruzi* and *T. brucei* as identified by the alignment of their amino-acid sequences with those of rabbit (Jeffery *et al.*, 2000), pig (Davies & Muirhead, 2002), human (Cordeiro *et al.*, 2003) and *Bacillus* (Sun *et al.*, 1999), the crystal structures of which have been described previously. This pattern of conserved residues suggests that the kinetoplastid PGIs share a common reaction mechanism with other PGIs. Nevertheless, differences can be observed between the mammalian and parasitic enzymes. A detailed comparison of the human and *Leishmania* PGI structures is critical to investigate whether these differences can be exploited in future structure-directed drug design.

In the present work, we describe the first successful expression, crystallization and preliminary X-ray characterization of the *Leishmania* PGI enzyme. For this purpose, two expression constructs were prepared, one containing the full-length gene (*PGI-Lm*) and a second construct (*dPGI-Lm*) in which the 5′ end of the gene that codes an N-terminal sequence unique to the *Leishmania* PGI was deleted. Hexagonal crystals with a large *c* unit-cell parameter were obtained and analyzed by X-ray diffraction. The initial phasing data for dPGI-Lm were obtained. Additionally, we have compared the inhibitory effects of four

phosphorylated compounds on human and *Leishmania* PGIs.

2. Material and methods

2.1. Subcloning *PGI-Lm* and *dPGI-Lm*

The *PGI-Lm* gene in the plasmid pBSIIKS(+) (Stratagene), as previously reported by Nyame *et al.* (1994), was used as starting material for our work. Oligodeoxynucleotide primers for PCR amplification (GIBCO-BRL) introduced *Nco*I and *Hin*dIII restriction sites at the 5′ and 3′ ends, respectively (5′-ACGG**CCATGG**GCGATTATTTTTCCAAATTGAAG-3′ for *Nco*I *PGI-Lm*, 5′-ACGG**CCATGG**GCCTGTTGCCTGCGTGG-3′ for *Nco*I *dPGI-Lm* and 5′-TCATGCA**AAGCTT**TTCACAGGTGTGCGCGAG-3′ *Hin*dIII for both constructs, *dPGI-Lm* and *PGI-Lm*) for cloning into pET28a(+) (Novagen). Two separate PCRs were used for the amplification of *PGI-Lm* and *dPGI-Lm*. Both reactions contained 2 pmol of each primer and approximately 50 ng of the pBSIIKS(+) containing the *PGI-Lm* open reading frame. The reactions were performed in a GeneAmp 2400 hermocycler (Perkin–Elmer CETUS) with 2.5 U of AmpliTaq DNA polymerase (Promega) according to the manufacturer's instructions. Each sample was subjected to 2 min denaturation at 367 K followed by 30 cycles of denaturation at 367 K for 0.5 min, annealing at 327 K for 0.5 min and extension at 345 K for 1 min. For each reaction, one DNA fragment of between 1.6 and 2.0 kbp was identified and gel purified with the Concert DNA-purification kit (GIBCO-BRL). Each purified DNA fragment was digested with the restriction enzymes *Nco*I and *Hin*dIII and ligated into the pET28a(+) vector previously digested with *Nco*I and *Hin*dIII. *Escherichia coli* BL21(DE3) competent cells were transformed with the products of the ligation reactions. Both cloned amplified forms of the *PGI* gene were sequenced with an ABI377 DNA sequencer to confirm their identity.

Cells from single colonies transformed with distinct vector constructs (*PGI-Lm* and *dPGI-Lm*) were grown overnight at 310 K at 250 rev min^{-1} in 5 ml LB medium containing 100 µg ml^{-1} kanamycin. These cultures were used as an inoculum to 250 ml 2×YT media containing 100 µg ml^{-1} kanamycin and grown at 310 K at 250 rev min^{-1} until $OD_{600\,nm}$ = 0.6. The cultures were then induced for expression of recombinant protein for 4 h with 0.5 m*M* isopropyl-β-D-thiogalactopyranoside (IPTG).

The *E. coli* BL21(DE3) cells were harvested by centrifugation at 6000*g* for 20 min. The cell pellet was suspended in 5 ml 50 m*M* HEPES pH 7.5 (buffer *A*) and cell lysis was obtained by the addition of lysozyme (0.5 mg ml^{-1}) and repeated freeze–thaw cycles. The crude extract was clarified by centrifugation (6000*g*, 20 min) and brought to 40%(*w*/*v*) and 50%(*w*/*v*) ammonium sulfate for 30 min with slow agitation at 277 K for dPGI-Lm and PGI-Lm, respectively. Each suspension was separated by centrifugation at 20 000*g* for 20 min and the supernatant was submitted to a final precipitation step with 70%(*w*/*v*) ammonium sulfate for both dPGI-Lm and PGI-Lm as described above. Each pellet was suspended in 5 ml buffer *A* and dialyzed against 250 ml of the same buffer with two buffer exchanges. Both PGI preparations were loaded (in separate runs) onto a 10 ml Q-Sepharose HP column equilibrated with buffer *A* and eluted in approximately 0.3 *M* NaCl in a linear gradient of buffer *B* (buffer *A* plus 1 *M* NaCl). Both recombinant *Leishmania* PGI proteins were dialyzed against 25 m*M* HEPES, 0.15 *M* NaCl pH 7.5 and applied (in separate runs) to a 115 ml Superdex-200 column equilibrated in the same buffer; the protein elution was checked by 15% SDS–PAGE. Concentration of both PGI forms to 5 mg ml^{-1} and buffer dilutions were performed by ultrafiltration using Centriprep30 and Centricon10 (Millipore). The isoelectric point for the recombinant PGIs was determined by gel isoelectric focusing in the pH range 3–9 (PhastSystem, Pharmacia).

2.2. Enzyme kinetics

Values of the kinetic parameters K_M and V_{max} were determined using F6P as the substrate at room temperature (298 K) in 100 m*M* triethanolamine buffer pH 7.6, following the formation of NADPH at 340 nm for 1 min in a coupled assay with glucose-6-phosphate dehydrogenase (Cracey & Tilley, 1975). Four PGI inhibitors analogous to reaction intermediates were evaluated and the measured IC_{50} values were determined at an F6P concentration of 800 µ*M* for both *Leishmania* and recombinant human PGI.

2.3. Sequence alignment

The amino-acid sequences of PGI-Lm (P42861) and its homologues from *T. brucei* (P13377; Marchand *et al.*, 1989) and *T. cruzi* (AAN78341; Andersson *et al.*, 1998) were obtained from the Swiss-Prot/TrEMBL database. Rabbit, human and *B. stearothermophilus* PGI sequences were obtained from the Protein Data Bank (PDB). The sequences were aligned using *CLUSTALW* (Thompson *et al.*, 1994). Further manual refinements were performed to optimize the alignment, taking the predicted secondary structure obtained from the individual polypeptides into consideration. Based on the recently proposed reaction mechanism described for rabbit PGI (Lee *et al.*, 2001; Arsenieva *et al.*, 2002; Jeffery *et al.*, 2001), functional residues were assigned.

2.4. Crystallization, X-ray diffraction data collection and initial phasing

Crystallization conditions for both dPGI-Lm and PGI-Lm were initially screened by the hanging-drop vapour-diffusion method using the sparse-matrix kits Crystal Screen and Crystal Screen II from Hampton Research at 291 K. 3 µl of protein solution at a concentration of 5 mg ml^{-1} in 6.25 m*M* HEPES, 37.5 m*M* NaCl pH 7.5 was mixed with an equal volume of well solution (0.5 ml per well) to form the drop. Screening different concentrations of precipitating agent and pH values further optimized the initial crystallization conditions. The best crystallization condition for both PGI-Lm and dPGI-Lm was obtained with a reservoir solution containing 10% polyethylene glycol 6000 (PEG 6000), 0.1 *M* Bicine pH 9.0 in a drop mounted as described above.

Crystals were mounted in nylon loops (Hampton Research) after quick soaking in a cryoprotectant solution consisting of the reservoir solution and 17.5%(*w*/*v*) methyl pentanediol (MPD). A complete data set consisting of 240 frames was collected from a single crystal of dPGI-Lm at the Protein Crystallography Beamline at the National Synchrotron Light Laboratory (Polikarpov *et al.*, 1998) using monochromatic X-rays of λ = 1.5450 Å at 110 K. The crystal-to-detector distance was 170 mm and each frame was exposed for 40 s with a 0.75° φ-angle oscillation. The *MOSFLM* package (Leslie, 1992) was used for autoindexing, data-collection strategy and image integration. Scaling and merging of reflections was performed using *SCALA* from the *CCP*4 package (Collaborative Computational Project, Number 4, 1994); the Matthews coefficient and solvent content were calculated using the program *MATTHEWS_COEF*, also from the *CCP*4 package. A homology-based model for dPGI-Lm was obtained from the SWISS-MODEL facility (Vagin & Teplyakov, 1997) using human PGI (PDB code 1jlh; Cordeiro *et al.*, 2001), which has 47.7% sequence

Table 1
IC_{50} values obtained in inhibition assays of human and *L. mexicana mexicana* PGI.

The inhibitors tested were 5-phospho-D-arabinonohydroxamic acid (5PAH), 5-phospho-D-arabinonate (5PAA), 5-phospho-D-arabinonamide (5PAAm) and 5-phospho-D-arabinonhydrazide (5PAHz).

	IC_{50} (μM)	
Inhibitor	hPGI	PGI-Lm
5PAH	16	50
5PAA	30	30
5PAAm	150	300
5PAHz	360	440

identity. This model was used for initial phasing by molecular replacement performed with the programs *AMoRe* (Navaza, 1997) and *MOLREP* (Vagin & Teplyakov, 1997). With the *AMoRe* routine, 18 887 unique reflections were used in the resolution range 30–3.5 Å; with the *MOLREP* routine, a total of 18 912 unique reflections were used to a maximum resolution of 3.5 Å. Both methods (*AMoRe* and *MOLREP*) resulted in equivalent solutions. Rigid-body and simulated-annealing refinement were performed using *CNS* v.1.1 (Brünger *et al.*, 1998). The program *O* v.8 (Jones *et al.*, 1991) was used to visualize the structure and to plot map files.

3. Results and discussion

3.1. Purification

The two recombinant forms of *L. mexicana mexicana* PGI were purified by similar procedures composed of three steps: selective precipitation by ammonium sulfate, ion-exchange and size-exclusion chromatography. These procedures resulted in approximately 2 mg of pure PGI from a 500 ml culture. Expression of the protein without the N-terminal 48 residues of the wild-type enzyme results in a protein (named dPGI-Lm) that has lower solubility in the presence of ammonium sulfate, a more basic isoelectric point and a tendency to aggregate at concentrations higher than 1 mg ml^{-1}. In the first purification step, concentrations higher than 40%(*w*/*v*) ammonium sulfate resulted in the precipitation of dPGI-Lm, while the complete form, PGI-Lm, is soluble at up to 50%(*w*/*v*) ammonium sulfate. Isoelectric focusing experiments in the pH range 3–9 resulted in the separation of multiple bands for both PGI forms. The identity of each band was not determined, but since the preparation was of high purity we speculate that the pattern of band separation in the IEF experiment arises from different quaternary conformations. We observed that the bands of PGI-Lm are spread over the pH range 5.2–5.8, while dPGI-Lm migrates as two bands at pH 6.0 and 6.4. This difference can be attributed to the elimination of the charged amino acids located in the N-terminus of PGI-Lm. The slightly acidic pI of 6.6 previously calculated from the amino-acid sequence (Nyame *et al.*, 1994) is thus confirmed by our experimental results. A tendency to form aggregates at concentrations higher than 1 mg ml^{-1} was only observed for dPGI-Lm. Although part of the purified dPGI-Lm was lost during concentration, it was possible to obtain a solution at 5 mg ml^{-1} that was suitable for crystallization experiments.

3.2. Enzyme kinetics and inhibitor assays

The enzyme-kinetic experiments performed on both forms (PGI-Lm and dPGI-Lm) indicate that the specific activity of the N-terminally abbreviated enzyme (450 U mg^{-1}) is not altered compared with that of the full-length form. Moreover, dPGI-Lm seems to crystallize with a better intrinsic order than PGI-Lm (see §3.4), suggesting that a disordered conformation of the N-terminal sequence affects the crystal packing.

Under our conditions, the kinetic parameters of PGI-Lm differ significantly from those of the recombinant human PGI when using F6P as the substrate. The human PGI has K_M and V_{max} values of 99 μM and 22 μM min^{-1}, respectively, while the K_M and V_{max} values for recombinant PGI-Lm are 242 μM and 80 μM min^{-1}, respectively. This may be a consequence of the natural pH range for both enzymes. The human PGI has a peak activity at physiological pH (close to 7.5), while for the *Leishmania* enzyme this value is more basic (between 8 and 9; Nyame *et al.*, 1994).

Four competitive inhibitors are known for *T. brucei*, *B. stearothermophilus*, yeast and/or rabbit muscle PGIs (Chirgwin & Noltmann, 1975; Hardré *et al.*, 1998, 2000; Hardré & Salmon, 1999). These inhibitors, namely 5-phospho-D-arabinonohydroxamic acid (5PAH), 5-phospho-D-arabinonate (5PAA), 5-phospho-D-arabinonamide (5PAAm) and 5-phospho-D-arabinonhydrazide (5PAHz),

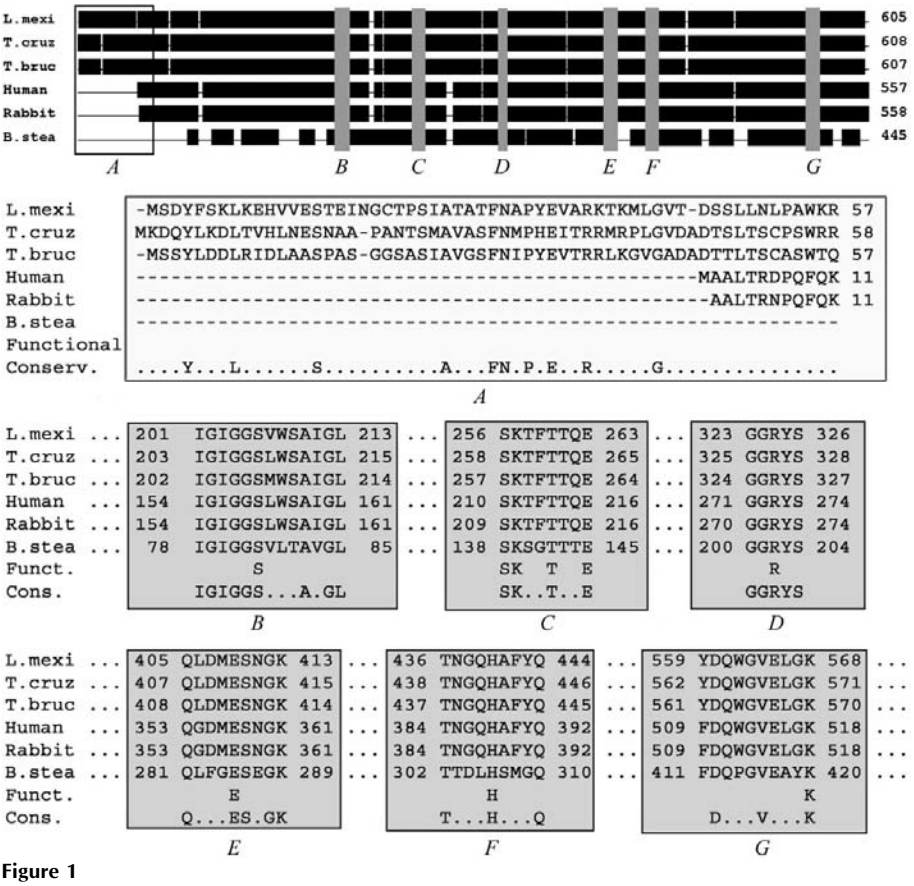

Figure 1
The top part of the figure represents a general view of the alignment of several PGIs of known three-dimensional structure [rabbit PGI (PDB code 1koj), human PGI and *B. stearothermophilus* PGI (PDB code 2pgi)] aligned with the *Leishmania mexicana*, *Trypanosoma brucei* and *T. cruzi* sequences. The position of conserved regions is indicated by boxes marked *A*–*G*. Those regions (*A*–*G*) are shown in more detail in the lower part.

were evaluated on the recombinant human and *L. mexicana mexicana* PGIs for comparative purposes (Table 1). To our knowledge, these compounds represent the first inhibitors to be evaluated on *L. mexicana mexicana* PGI. 5PAH and 5PAA have the highest IC_{50} values for both enzymes. Consistent with previously reported inhibition studies on the other PGIs, 5PAA and 5PAH behave as intermediate analogues of the isomerization reaction catalyzed by both the parasitic and human enzymes. In contrast, the IC_{50} values for 5PAAm and 5PAHz may indicate that these two compounds instead act as substrate-analogue inhibitors. Also, none of the four inhibitors show significant selectivity for the parasitic enzyme, a result consistent with the conserved active site as inferred from the sequence alignment. Furthermore, high-resolution crystal structures of PGIs in complex with the transition-state analogues 5PAA (Chou *et al.*, 2000; Jeffery *et al.*, 2001; Davies & Muirhead, 2002; Swan *et al.*, 2003) and 5PAH (Arsenieva *et al.*, 2002) highlight the structural conservation of the active-site region between those enzymes, except for *Pyrococcus furiosus* PGI (Swan *et al.*, 2003). Obviously, differences between the parasitic and human enzymes other than the active site would need to be taken into account for the further development of molecules of therapeutic interest. Nevertheless, these new inhibitors of the parasitic enzyme, especially 5PAH and 5PAA, can be considered as valuable tools for the future design of species-specific inhibitors of *Leishmania* PGI.

3.3. Sequence alignment

The multiple sequence alignment of PGI-Lm and its homologues adjusted with information from the available three-dimensional structures permitted the identification of highly conserved regions (illustrated as grey boxes in Fig. 1). Box *A* shows the N-terminal sequence that is restricted to Kinetoplastida. Boxes *B* and *C* show the regions next to the active site containing functional residues that are associated with the coordination of the substrate phosphate group in rabbit PGI (Lee *et al.*, 2001). Box *D* highlights a conserved peptide containing an arginine residue that acts like an anchor, stabilizing the non-reactive substrate analogue 6-phospho-D-gluconate (Jeffery *et al.*, 2000). In the presence of the substrate this arginine stabilizes the transient charge of a glutamic acid (in box *E*) during the isomerization step (Lee *et al.*, 2001). A histidine (box *F*) and lysine (box *G*) act in the ring-opening step prior to the isomerization step (Lee *et al.*, 2001).

Table 2
Statistics of the data set obtained from a single dPGI-Lm crystal and processed with *SCALA*.

Shell resolution (Å)	Reflections	Completeness (%)	Multiplicity	R_{sym}	$\langle I \rangle$	$I/\sigma(I)$
10.55	727	99.5	9.9	0.07	252	7.8
7.46	1284	100	9.8	0.08	203	4.7
6.09	1674	100	7.7	0.12	73	5.8
5.28	1957	99.8	6.4	0.13	67	5.2
4.72	2198	99.5	5.5	0.12	90	5.9
4.31	2416	99.2	5.1	0.13	81	5.1
3.99	2642	99.2	5.1	0.16	65	4.1
3.73	2832	99.1	5.3	0.22	45	3.1
3.52	3010	98.9	5.3	0.3	33	2.4
3.34	2806	88.2	3.9	0.48	20	1.5
Overall	21546	97.7	5.8	0.13	20.5	4.1

3.4. Crystallization, data collection and initial phasing

Crystals of both forms of *Leishmania* PGI have the same morphology. They grow as bipyramids with a hexagonal base and tend to be longer when grown using PEG 6000 concentrations of higher than 12.5% (Fig. 2). Comparing the diffraction pattern of crystals from both *Leishmania* PGI constructs grown under equivalent conditions, we realised that the crystals of dPGI-Lm presented a better intrinsic order, resulting in a larger number of reflections in the higher resolution shells, better defined reflection spots and a higher signal-to-noise ratio compared with the full-length PGI-Lm crystals. Although data from both crystals could be indexed, only the dPGI-Lm data resulted in a complete data set with acceptable statistical parameters. The crystals of both PGI-Lm and dPGI-Lm were best described by the primitive hexagonal crystalline system, with unit-cell parameters $a = b = 87.0$, $c = 354.7$ Å, $\alpha = \beta = 90$, $\gamma = 120^\circ$. In order to avoid overlaps in the spots, we tried to orient the crystal *c* axis perpendicularly to the direction of the X-ray beam and parallel to the φ rotation direction and set the crystal-to-detector distance to 170 mm. At this distance, the maximum resolution at the border of the detector was 3.3 Å (Fig. 3). Integrating and merging of 240 frames produced a total of 21 546 unique reflections in the resolution range 74.5–3.3 Å. A more detailed analysis of the reflection quality by resolution shell is presented in Table 2.

The autoindexing routine of the *MOSFLM* program suggested a primitive hexagonal lattice for the dPGI-Lm crystal. The observed multiplicity of 6 for the 00*l* reflections is associated with a screw axis (6_1

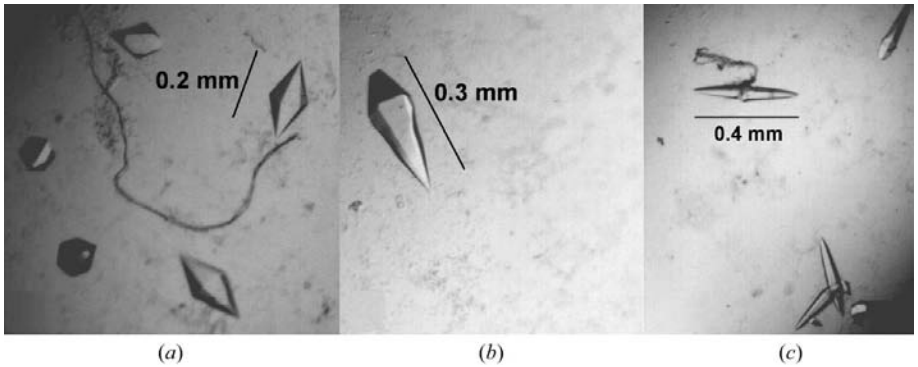

Figure 2
Crystals obtained from the dPGI-Lm constructs. These crystals were grown at pH 9.0 in 100 m*M* Bicine buffer and different concentrations of PEG 6000: (*a*) 10, (*b*) 12.5 and (*c*) 15%(*w*/*v*).

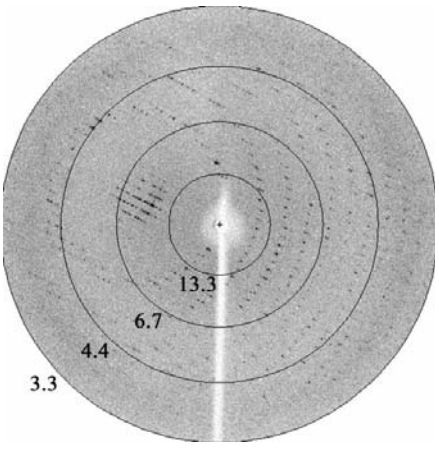

Figure 3
Diffraction image of PGI-Lm crystal on a MAR CCD detector.

or 6_5) and removed any possibility of a primitive trigonal group. Reasonable values of the Matthews coefficient (3.2 Å^3 Da^{-1}) and solvent content (61.6%) are predicted for a homodimer of dPGI-Lm in the asymmetric unit of space group $P6_1$ or $P6_5$. The application of molecular-replacement procedures for both possibilities indicated $P6_1$ to be the correct space group.

Initial phasing for one homodimer in space group $P6_1$ was performed separately using the *MOLREP* and *AMoRe* programs, resulting in equivalent solutions for the rotation and translation functions. The three highest *AMoRe* solution peaks present correlation coefficients of 50.4, 33.5 and 33.7. The highest peak is clearly a distinct solution described by rotational and translational vectors of 313.1, 113.9, 12.3 (Euler angles φ, θ, ψ) and 13.9, 42.0, 1.4 (x, y, z), respectively. Rigid-body and initial simulated-annealing refinement resulted in a dimer of dPGI-Lm in the asymmetric unit with an R factor of 0.27 and an $R_{\rm free}$ of 0.33. Continuous electron density is visible for all backbone atoms, allowing the orientation of inserted loops in dPGI-Lm that do not exist in the mammalian PGI structures. Future efforts will be made to grow crystals with better intrinsic order and higher resolution.

This work was supported in part by research grants 98/14979-7 from FAPESP and 478127/01-4 from CNPq to OHT. ATC is the recipient of a FAPESP student fellowship (Project No. 00/14960-6). We would like to thank the members of the Protein Crystallography and Structural Biology Group (IFSC-USP) for helpful discussions during the course of this work.

References

Andersson, B., Aslund, L., Tammi, M., Tran, A. N., Hoheisel, J. D. & Pettersson, U. (1998). *Genome Res.* **8**, 809–816.
Arsenieva, D., Hardré, R., Salmon, L. & Jeffery, C. J. (2002). *Proc. Natl Acad. Sci. USA*, **99**, 5872–5877.
Brünger, A. T., Adams, P. D., Clore, G. M., DeLano, W. L., Gros, P., Grosse-Kunstleve, R. W., Jiang, J.-S., Kuszewski, J., Nilges, M., Pannu, N. S., Read, R. J., Rice, L. M., Simonson, T. & Warren, G. L. (1998). *Acta Cryst.* D**54**, 905–921.
Chirgwin, J. M. & Noltmann, E. A. (1975). *J. Biol. Chem.* **250**, 7272–7276.
Chou, C.-C., Sun, Y. J., Meng, M. & Hsiao, C.-D. (2000). *J. Biol. Chem.* **275**, 23154–23160.
Collaborative Computational Project, Number 4 (1994). *Acta Cryst.* D**50**, 760–763.
Cordeiro, A. T., Godoi, P. H., Delboni, L. F., Oliva, G. & Thiemann, O. H. (2001). *Acta Cryst.* D**57**, 592–595.
Cordeiro, A. T., Godoi, P. H. C., Silva, C. H. T. P., Garratt, R. C., Oliva, G. & Thiemann, O. H. (2003). *Biochim. Biophys. Acta*, **1645**, 117–122.
Cracey, R. W. & Tilley, B. E. (1975). *Methods Enzymol.* **41**, 392–400.
Davies, C. & Muirhead, H. (2002). *Proteins Struct. Funct. Genet.* **50**, 577–579.
Hardré, R., Bonnette, C., Salmon, L. & Gaudemer, A. (1998). *Bioorg. Med. Chem. Lett.* **8**, 3435–3438.
Hardré, R. & Salmon, L. (1999). *Carbohydr. Res.* **318**, 110–115.
Hardré, R., Salmon, L. & Opperdoes, F. R. (2000). *J. Enzyme Inhib.* **15**, 509–515.
Jeffery, C. J., Bahnson, B. J., Chien, W., Ringe, D. & Petsko, G. A. (2000). *Biochemistry*, **39**, 955–964.
Jeffery, C. J., Hardré, R. & Salmon, L. (2001). *Biochemistry*, **40**, 1560–1566.
Jones, T. A., Zou, J.-Y., Cowan, S. W. & Kjeldgaard, M. (1991). *Acta Cryst.* A**47**, 110–119.
Lee, J. H., Chang, K. Z., Patel, V. & Jeffery, C. J. (2001). *Biochemistry*, **40**, 7799–7805.
Leslie, A. G. W. (1992). *Jnt CCP4/ESF–EAMCB Newsl. Protein Crystallogr.* **26**, 27–33.
Marchand, M., Kooystra, U., Wierenga, R. K., Lambeir, A. M., Van Beeumen, J., Opperdoes, F. R. & Michels, P. A. (1989). *Eur. J. Biochem.* **184**, 455–464.
Michels, P. A. M., Hannaert, V. & Bringaud, F. (2000). *Parasitol. Today*, **16**, 482–489.
Navaza, J. (1997). *Methods Enzymol.* **276**, 581–594.
Nyame, K., Do-Thi, C.-D., Opperdoes, F. R. & Michels, P. A. M. (1994). *Mol. Biochem. Parasitol.* **67**, 269–279.
Polikarpov, I., Perles, L. A., de Oliveira, R. T., Oliva, G., Castellano, E. E., Garratt, R. C. & Craievich, A. (1998). *J. Synchrotron Rad.* **5**, 72–76.
Readmond, S., Vadivelu, J. & Field, M. C. (2003). *Mol. Biochem. Parasitol.* **128**, 115–118.
Sun, Y. J., Chou, C. C., Chen, W. S., Wu, R. T., Meng, M. & Hsiao, C. D. (1999). *Proc. Natl Acad. Sci. USA*, **96**, 5412–5417.
Swan, M. K., Solomons, J. T. G., Beeson, C. C., Hansen, T., Schönheit, P. & Davies, C. (2003). *J. Biol. Chem.* **278**, 47261–47281.
Thompson, J. D., Higgins, D. G. & Gibson, T. J. (1994). *Nucleic Acids Res.* **22**, 4673–4680.
Vagin, A. & Teplyakov, A. (1997). *J. Appl. Cryst.* **30**, 1022–1025.